



HAL
open science

Modeling of pipeline corrosion degradation mechanism with a Lévy Process based on ILI (In-Line) inspections

Rafael Amaya-Gómez, Javier Riascos-Ochoa, Felipe Munoz, Emilio Bastidas-Arteaga, Franck Schoefs, Mauricio Sánchez-Silva

► To cite this version:

Rafael Amaya-Gómez, Javier Riascos-Ochoa, Felipe Munoz, Emilio Bastidas-Arteaga, Franck Schoefs, et al.. Modeling of pipeline corrosion degradation mechanism with a Lévy Process based on ILI (In-Line) inspections. International Journal of Pressure Vessels and Piping, In press, 10.1016/j.ijpvp.2019.03.001 . hal-02087291

HAL Id: hal-02087291

<https://hal.science/hal-02087291>

Submitted on 2 Apr 2019

HAL is a multi-disciplinary open access archive for the deposit and dissemination of scientific research documents, whether they are published or not. The documents may come from teaching and research institutions in France or abroad, or from public or private research centers.

L'archive ouverte pluridisciplinaire **HAL**, est destinée au dépôt et à la diffusion de documents scientifiques de niveau recherche, publiés ou non, émanant des établissements d'enseignement et de recherche français ou étrangers, des laboratoires publics ou privés.

Please cite this paper as:

Amaya-Gómez R, Riascos-Ochoa J, Muñoz F, Bastidas-Arteaga E, Schoefs F, Sánchez-Silva M. (2019). Modeling of pipeline corrosion degradation mechanism with a Lévy Process based on ILI (In-Line) Inspections. International Journal of Pressure Vessels and Piping, In press <https://doi.org/10.1016/j.ijpvp.2019.03.001>

Modeling of pipeline corrosion degradation mechanism with a Lévy Process based on ILI (In-Line) Inspections

Rafael Amaya-Gómez^{a,d,*}, Javier Riascos-Ochoa^c, Felipe Muñoz^a, Emilio Bastidas-Arteaga^d, Franck Schoefs^d, Mauricio Sánchez-Silva^b

^aChemical Engineering Department, Universidad de los Andes, Cra 1E No. 19A-40, Bogotá, Colombia

^bDepartment of Civil & Environmental Engineering, Universidad de los Andes, Cra 1E No. 19A-40, Bogotá, Colombia

^cBasic Sciences Department, Universidad Jorge Tadeo Lozano, Cra 4 No. 22-61, Bogotá, Colombia

^dUniversité de Nantes, GeM, Institute for Research in Civil and Mechanical Engineering/Sea and Littoral Research Institute, CNRS UMR 6183/FR 3473, Nantes, France

Abstract

In pipelines, one of the primary testing procedures used to identify the effects and evolution of corrosion over time is through In-Line Inspections (ILI). ILI inspections provide detailed information regarding the inner and outer pipeline condition based on the remaining wall thickness. Based on this information, different approaches have been proposed to predict the degradation extent of the defects detected. However, these predictions are subject of uncertainties due to the inspection tool and the degradation process that poses some challenges for assessing an entire pipeline within the timespan between two inspections. To address this problem, ILI data was used to formulate a degradation model for steel-pipe degradation based on a Mixed Lévy Process. The model combines a Gamma and Compound Poisson Processes aimed for a better description of the degradation reported by the ILI data. The model seeks to estimate corrosion lifetime distribution and the mean time to failure (MTTF) more accurately. The model was tested on an actual segment of an oil pipeline, and the results have been used to support a preventive maintenance program.

Keywords: Pipeline, corrosion, Mixed degradation process, Lévy Process, Maintenance.

1. Introduction

Corrosion is one of the frequent causes of failure in hydrocarbon pipelines [1, 2]. It follows a progressive degradation process in which the condition of the structure decreases continuously with time. Existing approaches to evaluate corrosion-based degradation include: (i) phenomenological descriptions [3, 4], (ii) random variable adjustments [5, 6], (iii) stochastic processes [7, 8], (iv) simulation processes [9, 10], (v) empirical approaches [11, 12], and (v) deterministic approaches [13]. Considering any of these degradation processes, the main challenge of a corrosion assessment lies in predict the condition of the pipeline between scheduled inspections to prevent any possible failure. Considering the nature of the transporting fluids, a loss of

*Corresponding author, Tel. (+57-1) 3394949 Ext.3095

Email address: r.amaya29@uniandes.edu.co (Rafael Amaya-Gómez)

containment may lead to human, environmental or economic losses. An important challenge relies on accounting for several factors that impact corrosion evolution, among them: current state, temperature, degradation initiation, and chemical composition of the steel.

For this purpose, pipeline integrity management practices such as the definition of inspection-repair strategies and failure analysis are commonly implemented. Within these practices, In-Line Inspection (ILI) assessment (NACE RP0102-2002 Standard) is a non-destructive technique often used to establish a clear perspective of the inner and outer condition of the pipe using magnetic (MFL) or ultrasonic (UT) tools to identify and measure metal loss. This analysis is commonly preferred from other acceptable methods reported in the Code of Federal Regulation for Liquids and Gases (CFR 192 and 195) to assess the mechanical integrity of pipelines [14]. The results of an ILI inspection are central to define a maintenance policy based on the pipeline condition [7, 15–17]. Overall, these policies seek to minimize the total expected life-cycle costs (i.e., construction, inspections, failures, and repairs) based on continuous degradation models.

Detailed assessments for long pipelines poses some restrictions on the selection of the evaluation tool. For instance, phenomenological approaches such as Computational Fluid Dynamics (CFD) or finite element analysis (FEM) require significant computational resources, which make impossible to assess all detectable defects in a system. Empirical and deterministic approaches do not capture the evolution of degradation mechanisms and their corresponding uncertainties. Simulation approaches such as Neural Networks require previous knowledge of distributions or data and lead to significant computational cost. Within this context, a stochastic based degradation can be used in advance as a way to handle both the degradation mechanism and the uncertainties associated with the ILI measurements.

Stochastic processes are justified by the fact that modeling degradation is a time-dependent process, which is uncertain by nature. The first approach in this direction corresponds to the use of Markov Chain processes. Some examples of this approximation include: (i) a model of the corrosion defect's effect on the remaining pipeline strength [18] and (ii) a model for pitting corrosion using non-homogeneous linear growth Markov process [19]. A second approach is the use of Gamma Processes as in Zhou et al. [20], in order to evaluate time-dependent pipeline reliability based on multiple active corrosion defects. This process has shown interesting results for predicting degradation in steel structures and life-cycle performance analyses [21, 22]. Finally, the use of Lévy Processes has attracted much attention recently [23, 24]. Based on a Lévy subordinator (i.e., increasing sample paths) as a Compound Poisson Process, degradation mechanisms can be best-described [23]. Recently, Riascos-Ochoa et al. [24] developed a model following a Lévy Process based on multiple degradation sources, which is then used to determine the Mean Time to Failure (MTTF) and Reliability by analytical expressions. In this work, this approach is used to assess the corrosion degradation process.

The objective of this paper is to present a stochastic characterization of a corrosion degradation process, which incorporates both the physical mechanism and associated uncertainties, with the aim to support operational decisions. The document is structured as follows: Section 2 presents a description of the evaluation of a pipeline performance over time. Section 3 describes the available degradation models for a corroded pipeline. Section 4 describes the proposed approach for modeling and assessing the reported corrosion. Section 5 presents the description of the case study; the results and discussion are shown in Section 6; and finally conclusions are given in Section 7.

2. Evaluation of pipeline performance over time

2.1. Inspection framework and underlying uncertainties

According to the Pipeline Operators Forum (POF), the result of an ILI inspection contains a pipe tally, list of anomalies, and a list of clusters [25]. The pipe tally presents a list of all pipeline and anomaly features, which include: (i) Location and orientation parameters, (ii) structural parameters, and (iii) information regarding anomalies. The list of anomalies describes the anomalies found with the inspection tool concerning their geometric extent (i.e., width, length, and depth), location, and orientation using a clock-position analogy (Fig. 1). Finally, a defect-cluster classification is provided in the list of defects considering the ASMEB31G criterion [25].

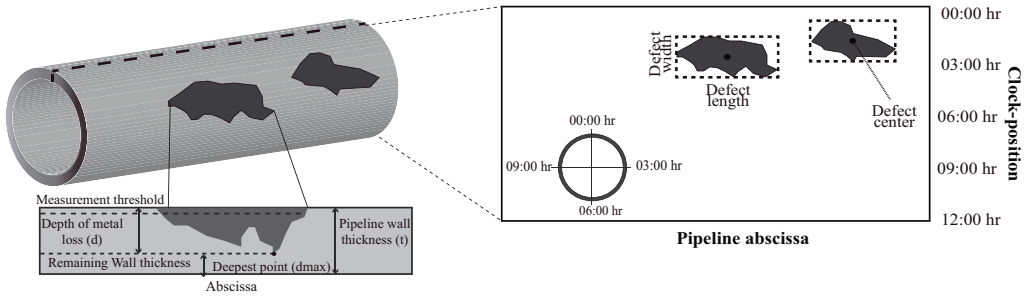


Figure 1: Scheme of the location of a corrosion defect. Modified from [25].

Specifically for metal loss assessment, ILI inspections capture information using Magnetic Flux Leakage (MFL) or Ultrasonic (UT) tools. The MFL tool induces a magnetic flux on the pipe wall seeking for flux leakages when the PIG (Pipeline Inspection Gauge) crosses the pipe. Based on the shape and amplitude of the signal, the nature of the anomaly can be estimated. The UT tool uses the time-elapsing reflexion and the angle of ultrasound waves to detect the metal loss [26]. As any other inspection tool, these techniques are subject to limitations detecting and measuring the corrosion defects on the pipe wall. For instance, MFL tools are primarily sensitive to the depth and the circumferential extent of an anomaly. However, long narrow areas of metal loss or axial cracks cannot be detected because the flux field is parallel to the length of the anomaly and the flux is not pushed outside of the wall thickness [26]. About the UT tool, several types of flaws including cracks or material separation are also detected [26], but this tool does not detect cracks with a length shorter than 30 mm or corrosion defects with a depth shorter than 2 mm [27].

Based on the inspection tool, each defect can be classified as detected or non-detected based on reporting thresholds that depend on the geometry of the defect (usually the depth). However, this detection process goes beyond a threshold that discriminates whether a defect is detected or not. Indeed, there is a probability that a sensor detects a defect (PoD- Probability of detection) or to be just a False Alarm (PFA-Probability of false alarm). This probability is relevant because it can be used as reporting threshold when information about the tool is not available [25] For this purpose, an exponential function is commonly used to describe the probability of detection based on the defect size and the accuracy of the inspection tool:

$$PoD(d) = 1 - \exp(-qd) \quad (1)$$

where d is the defect depth and $1/q$ is the average depth of defects that are detected [28]. Kwniewski et al. [29] proposed another approach to estimate this probability of detection. Based on laboratory hit-miss data, they suggested a fit with a log-logistic regression model with the following shape:

$$PoD(d) = \frac{\exp(b_0 + b_1 \ln(d))}{1 + \exp(b_0 + b_1 \ln(d))} \quad (2)$$

where $b_0 \in \mathbb{R}$ and $b_1 > 0$ are the fitting parameters.

Besides the PoD, the inspection results are delimited by the resolution of the inspection tool regarding the location and sizing of the defects. Table 1 illustrates the resolution from the principal measurement parameters reported by the Pipeline Operator Forum.

Table 1: Resolution of measurement parameters [25].

Parameter	Resolution/Accuracy	
	SI units	Alternative units
Abscissa	0.001 m	0.1 in
Defect length and width	1 mm	0.01 in
Defect depth	0.1 mm or 1%	0.01 in or 1%
Reference wall thickness	0.1 mm or 1%	0.01 in or 1%
Orientation	0.5 °C	1 minute
Temperature	1 °C	1 °F

Regarding defects dimension uncertainties, several authors have proposed random scattering errors associated with the ILI-reported dimensions, commonly normally distributed [6, 30, 31], and location uncertainties are associated with the inspection tool capabilities. ILI inspection contractor commonly provides information of the location and orientation capabilities of the inspection tool, namely, the axial position accuracy (in meters) and the circumferential position accuracy (in degrees).

2.2. Reliability problem formulation

Consider a system that starts operating at $t = 0$ and whose condition or capacity decreases with time. Denote this dependent time capacity at time t as V_t and let V_o denotes the initial capacity (i.e., at $t = 0$). The accumulated degradation at time t is described by a random variable X_t . In the case of pipelines, this condition can correspond to the remaining wall thickness. If the system is assumed to be abandoned after the first failure (i.e., without any maintenance), the system's condition at time t can be computed as [32]:

$$V_t = \max\{V_o - X_t, 0\} \quad (3)$$

The system failure occurs when its state falls below a predetermined ultimate or operational threshold k^* , where $0 < k^* < V_0$. An ultimate threshold corresponds to the case in which the system is unable to fulfill its function; for instance, the entire wall thickness of a pipeline. An operational threshold describes a minimum acceptable operative condition such as plastic deformation or a corrosion defect-depth of 80% of pipeline wall thickness. Depending on the implemented threshold, different possible interventions decisions can be supported. For instance, an ultimate threshold indicates that the system must be replaced, whereas an operational threshold suggests a preventive maintenance [33].

The following random variable can estimate the lifetime or the time in which the failure occurs:

$$L = \inf\{t \geq 0 : V_t \leq k^*\} = \inf\{t \geq 0 : X_t \geq V_0 - k^*\} \quad (4)$$

where $MTTF = \mathbb{E}[L]$, the reliability function is $R(t) = P(L > t) = P(V_t \geq k^*) = P(X_t \leq V_0 - k^*)$, and the failure probability writes $P_f(t) = 1 - R(t)$.

2.3. Degradation mechanisms

Degradation processes X_t are usually divided into three main categories: (i) shock-based, (ii) progressive, and (iii) combined degradation [24, 32, 33]. A shock-based degradation process occurs when discrete amounts of the system's capacity are removed at distinct points in time due to sudden and independent events (e.g., earthquakes). These shocks are assumed to occur randomly over time accordingly to some physical mechanism, and two stochastic processes describe them: (i) inter-arrival time between shocks $\{T_i\}_i^\infty$ and (ii) the damage of each shock $\{Y_i\}_i^\infty$. A particular case of a shock-based mechanism is a Compound Poisson Process (CPP), whose T_i are *iid* distributed exponentially. A progressive degradation (graceful) process is the result of the capacity being continuously reduced at a rate that may change over time. It is generally the result of a mechanical process based on internal or external conditions and can be described as a deterministic function rate or by progressive degradation jumps [33]. Finally, a combined degradation includes both processes. In what follows, some of the main stochastic approaches used to model the degradation process associated with corrosion will be presented.

3. Degradation models

Corrosion is a progressive degradation mechanism. Stochastic processes commonly used to model it are: the Gamma Process (GP) and the Inverse Gaussian Process (IGP). These are jump-processes with independent increments. The jumps are non-negative and happen infinitely often in any finite time interval, properties that makes these processes suitable to model progressive degradation. In fact in most cases, corrosion defects can be modeled rather accurately using a gamma distribution [5, 17, 20, 34, 35]. In what follows, the basic properties of these processes are briefly described below.

3.1. Gamma Process-based approach

According to van Noortwijk [36], a GP, $\{X_t\}_{t \geq 0}$, is a continuous stochastic process with the following properties: (i) $X_0 = 0$ with probability one, (ii) $X_\tau - X_t \sim Ga(v(\tau) - v(t), u)$ for $\tau > t \geq 0$, and (iii) X_t has independent increments. Here $Ga(\cdot, \cdot)$ denotes the gamma distribution given by:

$$Ga(x|v, u) = \frac{u^v}{\Gamma(v)} x^{(v-1)} e^{-ux} I_{(0, \infty)}(x) \quad (5)$$

where v and $u > 0$ are the shape and scale parameters, $I_{(0, \infty)}$ is the indicator function, and $\Gamma(v)$ is the Gamma function for $v > 0$. For the GP, $v(t)$ is non-decreasing function with continuous real values and $v(0) = 0$, which can be associated with a power law $v(t) = ct^b$ where $c, b > 0$ with a constant parameters b for corrosion modeling [37]. These parameters are commonly determined by statistical methods such as maximum likelihood and method of moments [36]. The GP lifetime can be expressed by the incomplete gamma function (i.e., $\Gamma(a, x) = \int_{t=x}^{\infty} t^{(a-1)} e^{-t} dt$) as follows [37]:

$$F(t) = P(L \leq t) = P(X_t \geq V_o - k^*) = \frac{\Gamma(v(t), (V_o - k^*)u)}{\Gamma(v(t))} \quad (6)$$

The lifetime probability density function (*pdf*) is obtained using the chain rule, assuming that $v(t)$ is differentiable [36]:

$$f(t) = \frac{v'(t)}{\Gamma(v(t))} \int_{(V_o - k^*)u}^{\infty} [\log(z) - \psi(v(t))] z^{v(t)-1} e^{-z} dz \quad (7)$$

where the function $\psi(a)$ corresponds to the digamma function.

3.2. Inverse Gaussian Process-based approach

The inverse Gaussian Process (IGP) is one of the stochastic processes recently implemented to model degradation processes [31, 38–41]. The IGP is a process with independent increments following an Inverse Gaussian distribution. It has the following properties [31]: (i) $X_0 = 0$ with probability one, (ii) $X_\tau - X_t$ follows an inverse Gaussian distribution with *pdf*: $f_{X_\tau - X_t}(x_\tau - x_t | \Lambda_\tau - \Lambda_t, \zeta(\Lambda_\tau - \Lambda_t)^2)$, and (iii) $\{X_t\}_t^\infty$ has independent increments.

If the mean of the distribution is denoted as $\mu > 0$ and the shape parameter is denoted as $\theta > 0$, then the IGP probability density function for a random variable X is given by [31]:

$$f_X(x | \mu, \theta) = \sqrt{\frac{\theta}{2\pi x^3}} \exp\left(-\frac{\theta(x - \mu)^2}{2\mu^2 x}\right), \quad x > 0$$

The corresponding variance for this *pdf* is given by μ^3/θ . Now, let $\{X_t\}_{t \geq 0}$ be a IGP over a time t . Then a parametrization with a mean function $\Lambda_t = \mathbb{E}[X_t]$ and a shape function $\zeta(\Lambda_t)^2$, where ζ is a scale parameter, obtain the *pdf* of the IGP process as follows [31, 41]:

$$f_{X_t}(x_t | \Lambda_t, \zeta(\Lambda_t)^2) = \sqrt{\frac{\zeta}{2\pi x_t^3}} \Lambda_t \exp\left(-\frac{\zeta(x_t - \Lambda_t)^2}{2x_t}\right), \quad x_t > 0, \quad (8)$$

which in turn, reaches the following reliability function given a threshold k^* [41]:

$$\begin{aligned} R(t) &= P(X_t \leq k^* | \Lambda(t), \zeta) \\ &= \phi \left[\sqrt{\frac{\zeta}{k^*}} (k^* - \Lambda(t)) \right] + \exp\{2\zeta\Lambda(t)\} \phi \left[-\sqrt{\frac{\zeta}{k^*}} (k^* + \Lambda(t)) \right]. \end{aligned}$$

For monotone degradations such as corrosion, this stochastic process is suitable because the monotonic requirement is inherently ensured. This requirement is completed thanks to the mean function, which is required to be monotonically increasing with time. Some approaches as Qin et al. [39] and Zhang & Zhou [31] suggest a power law function for this purpose:

$$\Delta\Lambda_{ij} = \begin{cases} \alpha_i(t_j - t_{i0})^\beta, & \text{for } j = 1 \\ \alpha_i(t_j - t_{j-1})^\beta, & \text{for } j \geq 2 \end{cases}$$

where t_{i0} is the initiation time of the i^{th} corrosion defect, t_i represents the time of the i^{th} inspection, α_i is the mean growth rate in a unit time, and β is a constant that delineate the power law performance of this function. From the approaches reviewed, this last parameter was set to $\beta = 1$, which represents a linear trajectory over time [31, 39, 40].

Some variations of the above approaches include: (i) a GP or an IGP with a Gaussian copula (or a sum of GPs or IGPs) to model the degradation of several corrosion defects [40], and (ii) an IGP with random effects to address common heterogeneities (random degradation rate) [38]. In general, these approaches fit the degradation process using the mean and variance (i.e., first two central moments); however, recent results have shown that also the third moment affects the fitting and poses additional challenges for the corrosion predictions [42].

3.3. Mixed process: A Lévy Process approach

One general stochastic process that includes GP and IGP is a Lévy Process, which is defined as follows [24]: Given a filtered probability space $(\Omega, \mathcal{F}, \mathbb{F}, \mathbb{P})$, an adapted process $\{X_t\}_{t=0}^{\infty}$ with $X_0 = 0$ almost surely (a.s.) is a Lévy process if:

- $\{X_t\}_t^{\infty}$ has independent increments from the past, namely, $X_t - X_s$ is independent from \mathcal{F}_s with $0 \leq s \leq t \leq \infty$
- $\{X_t\}_t^{\infty}$ has stationary increments, namely, $X_t - X_s$ has the same distribution as X_{t-s} with $0 \leq s \leq t \leq \infty$.
- X_t is continuous in likelihood, namely, $\lim_{t \rightarrow s} \mathbb{P}(X_t \in \cdot) = \mathbb{P}(X_s \in \cdot)$.

Using the Lévy-Ito decomposition theorem, it is possible to describe a Lévy Process as a superposition of three independent processes: (i) deterministic drift, (ii) quadratic Gaussian process, and (iii) a Lévy measure. Clearly, in the case of systems that degrade continuously, the second component (i.e., Gaussian quadratic part) can be neglected, and the process will still be Lévy. This process can be implemented through the *characteristic function* and the corresponding *characteristic exponent* of the three main degradation processes that can be described: (i) shock-based, (ii) progressive, and (iii) mixed-based (See Section 2.3).

A shock process, W_t , may be implemented if: (i) the deterministic drift is neglected; and (ii) the Lévy measure has support on \mathbb{R}^+ and it is finite. Thus, W_t corresponds to a CPP and can be written as $W_t = \sum_{i=1}^{N_t} Y_i$, where N_t is the number of shocks until time t . Consider the shocks following a Poisson process with rate λ . A progressive degradation corresponds to the sum of two independent processes: (i) a linear deterministic drift and (ii) a jump process with an infinite Lévy measure, i.e., $\Pi_Z(\mathbb{R}) = \infty$. The mean and the n -th central moment of Z_t would be given by the characteristic exponent of the jump process [24]. In the particular case of a GP, consider the shape function of the gamma distribution as $\nu(t) = \lambda_g t$ ($\lambda_g > 0$) and a scale parameter $u = \beta_g$. Finally, a Mixed-Lévy process K_t is defined as the sum of two independent models, and its characteristic exponent correspond to a linear combination of the constitutive processes. Based on the characteristic function, mean and central moments expressions of the degradation process can be determined by their n -th derivate evaluated at zero. Further details can be found in Riascos-Ochoa et al. [24]. The equations for the mean, variance, and third central moment of each process are summarized in Table 2.

Riascos-Ochoa et al. [24] proposed a numerical solution to obtain the reliability quantities (i.e., lifetime, MTTF, and reliability function) using the inversion formula. Appendix A presents an approach to determine the parameters, which will be later used for modeling corrosion.

Table 2: Mean, variance, and third central moment for Lévy Processes

Process	Mean	Variance	Third central moment
Shock-based W_t	$\mathbb{E}[W_t] = \lambda t \mathbb{E}[Y]$	$Var[W_t] = \mu_{(2,W)}(t) = \lambda t \mathbb{E}[Y^2]$	$\mu_{(3,W)}(t) = \lambda t \mathbb{E}[Y^3]$
Progressive (GP) Z_t	$\mathbb{E}[Z_t] = \lambda_g t / \beta_g$	$Var[Z_t] = \mu_{(2,Z)}(t) = \lambda_g t / \beta_g^2$	$\mu_{(3,Z)}(t) = 2\lambda_g t / \beta_g^3$
Mixed Process K_t	$\mathbb{E}[K_t] = \alpha_s \mathbb{E}[W_t] + \alpha_p \mathbb{E}[Z_t]$	$Var[K_t] = \alpha_s Var[W_t] + \alpha_p Var[Z_t]$	$\mu_{3,K}(t) = \alpha_s \mu_{3,W}(t) + \alpha_p \mu_{3,Z}(t)$

4. Approach to corrosion modeling and assessment

4.1. Overview

Overall, data collected with ILI inspections is used as the basis for modeling degradation due to corrosion, which is later used to evaluate the mechanical integrity of the pipeline. After collecting corrosion data from the ILI inspection, a tidying process that focused on the measurement of the defects and their location is carried out. Based on this information, a stochastic degradation model that captures the evolution of the corrosion-depth increments at various ILI measurements is constructed, the pipeline integrity is evaluated using the Mean Time to Failure along the abscissa to identify leak-prone segments and the potential spilled volume in case of a LOC to identify potential critical segments. Finally, an *Age Replacement Maintenance* comparison is implemented based on the proposed approach. Fig. 2 illustrates the overall methodology proposed in this work.

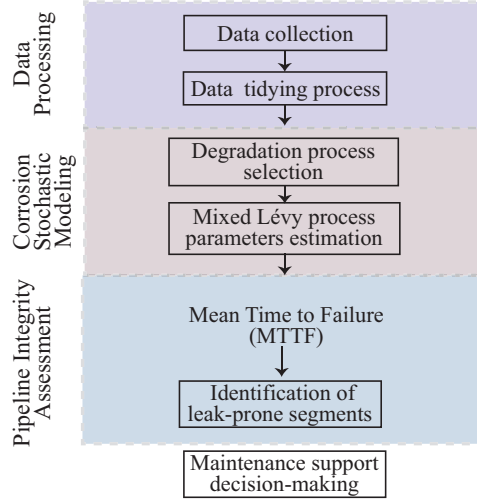


Figure 2: General methodology for pipeline degradation assessment.

4.2. Data processing

Assume initially that the ILI inspection tool has a defect location uncertainty denoted as ϵ , commonly reported by the inspection vendor. Which means that a defect $x = (x_1, x_2)$ may be

located within a circular area $\mathcal{B}_\epsilon(x) := \{y = (y_1, y_2) \in (\mathbb{A} \times \mathbb{P}) \mid \sqrt{(x_2 - y_2)^2 + (x_1 - y_1)^2} \leq \epsilon\}$, where $(\mathbb{A} \times \mathbb{P})$ is the ordered pair indicating the abscissa and perimeter defect location on the pipeline. This uncertainty is important considering that defects might not be accurately located between two ILI runs. Let's define S_1 as the set of depth increments at the exact location between ILI runs, and S_2 as the set of depth increments considering the possibility that there is some uncertainty in the location of the defect. In the former case, depth increments can be obtained directly from the measurements. However, in the latter case, more than one corrosion defect may be located in these circular regions. In this case, a hypothetical corrosion defect could be defined by the mean or maximum depth of the corrosion defects within each \mathcal{B} (Fig. 3).

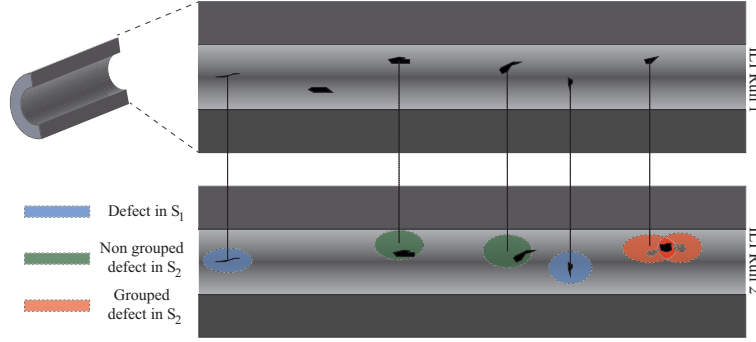


Figure 3: General S_1 and S_2 diagram.

4.3. Stochastic corrosion model

The proposed growth corrosion model is based on the geometric extent of defects, principally on depth-increments. Based on several ILI measurements, the corrosion evolution along the pipeline is determined from defect depth increments between inspections. If there are m detected defects and n ILI measurements, the depth increments δ_j^i of the i -th defect in the j -th inspection could be obtained by:

$$\begin{aligned} \Delta_x &= \{\delta_j^1, \dots, \delta_j^m\} \quad \forall j \in 2, 3, \dots, n \\ \Delta_x &= \{(x_j^1 - x_{j-1}^1), \dots, (x_j^m - x_{j-1}^m)\} \quad \forall j \in 2, 3, \dots, n \end{aligned} \quad (9)$$

where x_j^i denotes the degradation (e.g., defect depth) of the i -th defect at the j -th ILI measurement. The equations in Section 3 correspond to the degradation process of only one corrosion defect, and it should be implemented for each defect to evaluate the integrity of the entire pipeline. Nevertheless, this process may be unfeasible due to their computational cost considering that a pipeline of 45km might have more than 60,000 corrosion defects over a period of 50 years. The latter following the generation of new defects results of Zhang [7]. Therefore, it was assumed that every defect has the same degradation mechanism; the following two alternatives are proposed to determine their degradation parameters:

1. To consider the expected metal loss on the wall thickness on the corrosive location instead of individual corrosion increments $(x_j^i - x_{j-1}^i)$.

2. To consider all the corrosion increments ($x_j^i - x_{j-1}^i$) as two hypothetical ILI measurements with these increments.

In both alternatives, depth-increments are used as input to estimate the parameters. In this work, the latter case is implemented because two ILI measurements were available.

4.3.1. Selection of the degradation mechanisms

Based on the available ILI inspections, the degradation process that best describes its corrosion mechanism is determined using the *Feasible Moments Criterion* [24]. This criterion considers the second and third central moments (i.e., $\mu_2(t)$ and $\mu_3(t)$) of the degradation process, which increase proportionally with time (see Table 2); thus, $\mu_2(t)/t$ and $\mu_3(t)/t$ are constant parameters associated with the increasing rates of these moments. This criterion uses the ordered pairs $\{\mu_2(t)/t, \mu_3(t)/t\}$ to select the degradation mechanism that better fits the data. This paper proposes a Mixed Lévy process composed of a Gamma Process (GP) and a Compound Poisson Process (CPP) upon the results from the *Feasible Moments Criterion* just mentioned before (see Section 3.3).

Once the mechanisms are selected, the next step is to determine the parameters of these mechanisms. The progressive degradation mechanism follows a Gamma Process, $\{Z_t\}_{t \geq 0}$, which is also a Lévy Process, so its parameters can be determined based on the degradation mean and variance (see Appendix A). Note that the reported in Appendix A involve the mean and variance of the corrosion depth-increments, but does not depend on the third central moment, which is a measure of the degradation skewness. Once the parameters of the GP are defined, it remains to determine the shocks size (Y), the shocks time inter-arrival time (λ) of the shock process $\{W_t\}_{t \geq 0}$, and the superposition coefficients (α_s, α_p), which will depend on the shocks' distribution. These parameters are estimated using an optimization model that assumes that a previous moment-matching approach for progressive degradation is already completed (see Appendix A).

4.3.2. Optimization-based model

Consider that the mean and central moments of the shock-based process are described in terms of the shocks size (Y) and their inter-arrival time (λ). Also, assume that the corrosion depth-increments are independent. Then, the parameters can be obtained by minimizing the difference between the third moment of the degradation process with the actual reported data. This optimization should be subjected to fit the mean and second central moment of the depth-increments from the ILI measurements (\mathbb{E}_{ILI} and $\mu_{(2,ILI)}$):

$$\begin{aligned} & \underset{\{\alpha_p, \alpha_s, \lambda, Y\}}{\text{minimize}} && \left| \alpha_p \mu_{(3,Z_t)} + \alpha_s \mu_{(3,W_t)} - \mu_{(3,ILI)} \right| \\ & \text{subject to} && \alpha_p \mu_{(2,Z_t)} + \alpha_s \mu_{(2,W_t)} = \mu_{(2,ILI)} \\ & && \alpha_p \mathbb{E}_{Z_t} + \alpha_s \mathbb{E}_{W_t} = \mathbb{E}_{ILI} \end{aligned} \quad (10)$$

This approach assures that the degradation process describes the mean and central moments of the corrosion defects-depth increments completely.

4.4. Pipeline integrity assessment

Pipeline integrity comprises concepts of failure prevention, inspection, and repair, including products, practices, and services that help operators maximize their assets. Pipeline integrity evaluation is a problem commonly addressed in standards such as API579 (*Fitness-For-Service*), ASME B318S (*Managing System Integrity of Gas Pipelines*) and API1160 (*Managing system*

integrity for hazardous liquid pipelines). The main practices regarding pipeline integrity management can be found in Kishawy & Gabbar [43]. This paper proposes to evaluate the pipeline Mean time to Failure (MTTF), which is part of commonly reported statistical methods that are very attractive for decision makers [32]. MTTF is the expected time for a possible Loss of Containment (LOC) due to a corrosion defect. For the moment, this failure represents an ultimate limit state in which the wall thickness is entirely consumed by the corrosion degradation process. This paper does not contemplate other failures such as plastic collapse or deformation, which are reviewed in more detail in [44], but concentrates on the information that can be provided exclusively from the degradation process. Note that the evaluation of the MTTF requires the computation of the failure time distribution, which also provides valuable information on the degradation process and for pipeline reliability. In this paper, leak-prone segments were identified along the abscissa using the minimum MTTF for each of the pipeline sections regardless of their clock-position. Afterwards, the potential spill volume is estimated following the dynamic and static volumes reported in [45] assuming 5 minutes to stop the pipeline pumps given a LOC and using the nominal capacity of the pipeline. This information is then used to identify critical segments of the pipeline seeking to support a conservative intervention decision-making process, considering the minimum pipeline resistance and a possible replacement that withstand further corrosion depth-increments.

4.5. Maintenance application: Age-Replacement Model

The information obtained from the degradation process can be used to formulate a suitable pipeline maintenance strategy following the *Age Replacement Model*. This model focuses on preventive (i.e., before failure) and reactive or corrective (i.e., at failure) intervention times only, and not on the degradation process [32]. Thus, the system is replaced upon failure or when it reaches a predetermined critical age α (Fig. 4). This model is commonly used in case of an increasing failure rate, which applies to the case of pipelines.

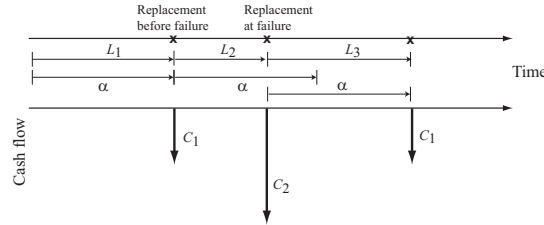


Figure 4: Age-Replacement Model representation. Modified from [32].

This maintenance policy assumes an immediate replacement and that any intervention would bring the system to its initial condition, i.e., *as good as new*. Let C_1 and C_2 denote the preventive and corrective maintenance costs, respectively, then $C_2 > C_1$. Let also L_t be the lifetime distribution of a new system with finite mean, then the sequence of replacement times constitute a renewal process, i.e., each cycle begins and ends with a replacement. The objective is to find the critical age α that minimize the expected cost per unit time for an infinite time horizon, $K(\alpha)$, which corresponds to the ratio between the expected cost in a cycle and the expected length of it. Recall that a planned replacement occurs if $L > \alpha$, otherwise a corrective replacement is used instead, then the expected cost per unit time is given by [32]:

$$K(\alpha) = \frac{C_1 \bar{L}_t(\alpha) + C_2 L_t(\alpha)}{\int_0^\alpha \bar{L}_t(u) du} \quad (11)$$

where $\bar{L}_t(\alpha) = \mathbb{P}(L > \alpha)$. Note that when $\alpha = \infty$ the policy has replacement only at failures and $K(\infty) = C_2/\mathbb{E}[L]$. The details of this type of maintenance can be found elsewhere [32]. For the particular case of a Lévy degradation process, Riascos-Ochoa [42] proposed a numerical solution to determine this optimal age based on the bisection method; the details of this approach will not be discussed in here.

5. Case of Study

5.1. Problem description

The case study evaluates a real carbon steel pipeline grade API5LX52 alloy; the pipeline characteristics are shown in Table 3. Two corrosion data sets were obtained from ILI measurements 2 years apart. In the first run, 33,466 defects were identified and in the second 59,101. For confidential agreements, further information about the case study cannot be provided.

Table 3: Pipeline summary parameters

Parameter	Value	Units
Outer diameter	273.1	mm
Nominal diameter	10	in
Pipeline length	44	km
MAOP (Maximum Allowable Operating Pressure)	1500	psig
SMYS (Specified Minimum Yield Strength)	52,000	psig
SMTS (Specified Minimum Tensile Strength)	60,000	psig
Average wall thickness	6.35	mm
Operating temperature range	303.55-307.05	K
Operating velocity range	1.7-2.4	m/s

Besides the information provided in Table 3, the distribution of the metal loss anomaly classification on the inner and outer walls was determined following the criteria defined by the Pipeline Operators Forum [25]. It was obtained that: (i) almost 50% of the defects are classified as pitting, and the remaining are distributed mainly in circumferential slotting, and (ii) the metal loss defects are mostly located in the inner wall with around 80% in both ILI measurements.

5.2. Data treatment

Changes in the depth of defects were assessed based on observations of the two ILI measurements, and the defects were treated independently. Besides, since the exact type of the MFL tool used for pipeline inspection was not known; then, an uncertainty of 5° in the circumferential location of the defects during the inspection was assumed based on the vendor reports as it was described in Amaya-Gómez et al. [5]. This uncertainty corresponds to 12 mm or a deviation of 5%, obtaining two different data sets: (i) defects with a depth change between the two ILI measurements located in the same position; and (ii) defects with location differences between the ILI measurements with a deviation less or equal to 5%. These sets are denoted as Set-1 and Set-2, respectively. Only defects with a correspondence between the two ILI measurements were taken into account; defects generated in the second inspection and those repaired have not been considered for this work

6. Results and discussion

6.1. Corrosion degradation model

Based on the two ILI inspections, depth-increments X_t were computed (Eq. 9) for both Set-1 and Set-2. Moreover, the GP parameters from both sets were determined using the equations reported in Table 2 for $t = 2$ and with $\mu_{2,X_t} = \text{Var}[X_t]$:

$$\lambda_g = \frac{(\mathbb{E}[X_t])^2}{\mu_{2,X_t} \cdot t} \quad \beta_g = \frac{\mathbb{E}[X_t]}{\mu_{2,X_t}} \quad (12)$$

The results are shown in Table 4. Despite the similarities between both sets, Set-2 includes depth-increments from Set-1. Considering the stationary assumption and a mean wall thickness of 6.35mm, the MTTF can be approximated linearly to 35.86 and 40.32 years for Set-1 and Set-2, respectively. Since this expected lifetime depends on the central moments of the degradation process [24], the MTTF obtained is conservative.

Table 4: GP Set-1 and Set-2 parameters

Set	$\mathbb{E}[X_t]/t$	$\mu_{2,X_t}/t$	λ_g	β_g
Set-1	0.1771	0.0325	0.9648	5.4477
Set-2	0.1575	0.0384	0.6456	4.0987

The *Feasible Moments Criteria* was implemented to select the degradation process that better describes the corrosion depth-increments using the second and third central moment [24]. The results indicate that a Mixed-Lévy Process with a GP as a progressive process and a shock-based process with shocks distributed as Delta-Dirac or Exponential should be considered. The corresponding mean and central moments for both distributions following the reported in Table 2 are [24]:

$$\begin{aligned} \mathbb{E}[W_t]_\delta &= \lambda t y, & \mathbb{E}[W_t]_{EXP} &= \lambda t y \\ \text{Var}[W_t]_\delta &= \lambda t y^2, & \text{Var}[W_t]_{EXP} &= 2 \lambda t y^2 \\ \mu_{(3,W_t)}|_\delta &= \lambda t y^3, & \mu_{(3,W_t)}|_{EXP} &= 6 \lambda t y^3. \end{aligned} \quad (13)$$

6.1.1. Optimization approach

Considering that the Set-1 is a subset of Set-2, the progressive degradation Z_t parameters were determined from the GP of the Set-1. Moreover, the mean and central moments from the ILI measurements were implemented in the proposed optimization process in Eq. 10. This equation was solved using the Matlab ®Pattern Search algorithm, obtaining the optimum parameters shown in Table 5. These parameters indicate that the GP contributes the most to the degradation process. Although the inter-arrival time rates between shocks are almost the same between both mixed processes, there is a significant difference between shock sizes.

Furthermore, the error obtained from the third central moment (μ_{3ILL}) is almost 0 for the Mixed GP+CPP- δ and GP+CPP-*Exp* processes (i.e., $1.4 \cdot 10^{-10}\%$ and $7.4 \cdot 10^{-11}\%$ respectively). In both cases, the result was lower than 5.09% from GP_{Set2}.

The *pdf* of the degradation distribution obtained using different models is presented in Fig.5 and it was compared with the data obtained from the ILI measurements. Although there are some discrepancies at lower corrosion values, in the tail of the distribution there is a good agreement between ILI data and the GP_{Set2} and both Mixed processes. The mean degradation (and coefficient of variation) for all models for $t = 2$ were: 0.3542 mm (0.720) for GP_{Set1}, 0.3151 mm

Table 5: Mixed process parameters by optimization

Mixed process	α_p	α_s	λ	y
GP-CPP (Delta)	0.774	0.071	0.447	0.648
GP-CPP (EXP)	0.616	0.569	0.448	0.190

(0.881) for GP_{Set2} , 0.3151 mm (0.881) for $GP-CPP-\delta$, and 0.3152 mm (0.883) for $GP-CPP-Exp$. The results from the mixed processes and the GP_{Set2} were closer to the obtained from the ILI Data: 0.3150 mm (0.902).

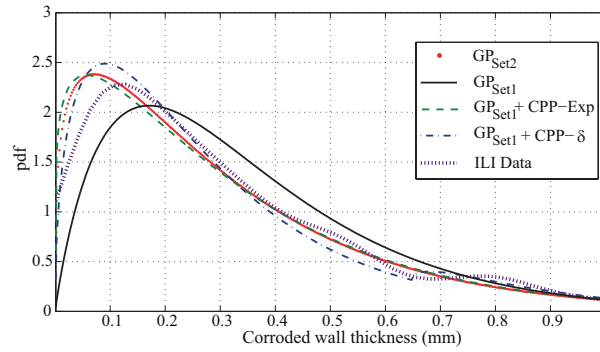


Figure 5: Corroded wall thickness probability density function.

6.2. Pipeline integrity assessment

Based on a numerical approach, the corresponding reliability quantities were determined [24]. The expected corroded depth-increment was 0.15mm/year and the MTTF of 41.08 years, which is consistent to the mean lifespan of a pipeline (i.e., near 35 years) and the mean degradation obtained in Amaya-Gómez et al. [5] for a plastic strain. In addition, the lifetime distribution for an intact pipeline in the Mixed Process is depicted in Fig. 6. Hereafter, the mixed process $GP+CPP-\delta$ is used to evaluate the pipeline integrity.

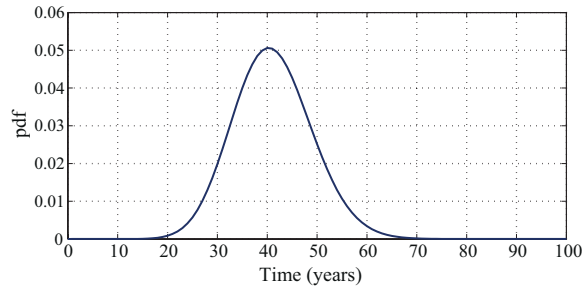


Figure 6: Lifetime distribution for the Mixed Process.

Assume that the pipeline is divided into equally spaced segments 1 m long each. The minimum MTTF over the entire clock position can be calculated using the $GP+CPP-\delta$ model for every segment. In this particular case study, three leak-prone sections were identified; they are

located at: (i) km-27+4, (ii) km-33+7 and (iii) km-40+9; being the latter, the most critical with an approximately MTTF of 12 years once the evaluation was addressed in the last ILI inspection. Besides, there is a pipeline segment around 43 km that has also reduced wall thickness. These sections were further studied in detail to provide a better insight into their criticality as it is shown in Fig. 7 using their potential spill volume. The results indicate that these sections may produce extreme spillages in case of a LOC (i.e., over 1000 bls) by assuming a pump stop time of 5 minutes and considering the static volume and the pipeline altimetry. Note that there are defects located near the 8th kilometer with a MTTF close to 20 years with potential spills under 500 bls, so these segments could be maintained after the three leak-prone sections aforementioned. The location of critical segments is important, but also the extent and type of defects. For example, once critical sectors are identified, possible interactions among the various defects within the segment could be evaluated.

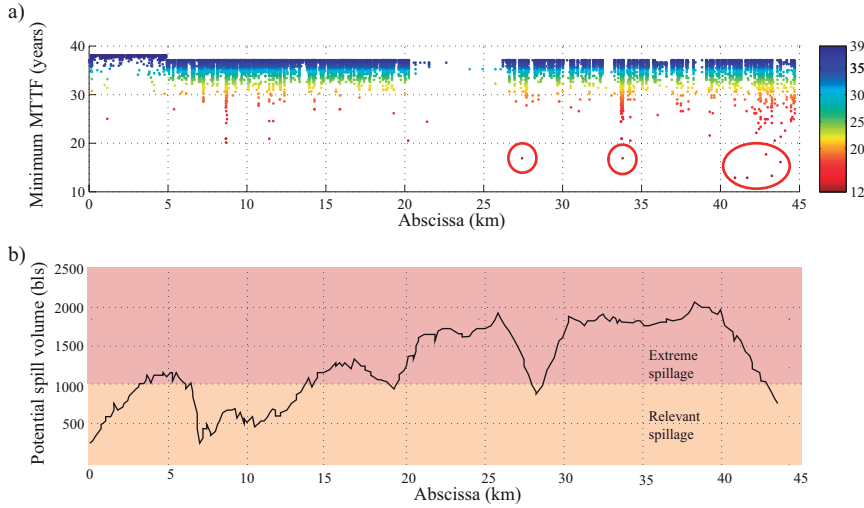


Figure 7: a) Minimum MTTF and b) potential spill volume results along abscissa.

6.3. Maintenance program

In this example, the inspection, excavation, repair, and replacement unit costs are typical values of the industry in Canada reported in Zhang & Zhou [7], which represents a maintenance cost of $C_1 = 80,000$ USD/Joint. For illustrative purposes, the replacement cost C_2 was selected from the following C_2/C_1 ratios: 2, 4, 6, 10, 20, 40, 60, and 100. Based on the numerical solution proposed in [42], the optimal replacement time was calculated for the four degradation processes discussed above; i.e., GP_{Set1} , GP_{Set2} , $GP_{Set1} + CPP - \delta$ and $GP_{Set1} + CPP - Exp$ (See Fig. 8). A clear dependence between this optimal age of replacement with the failure cost C_2 can be detected; namely, numerous inspections are required to avoid a costly failure. Besides, this figure shows that the results from the mixed processes and the GP_{Set2} are almost the same, whereas lower ages of replacement are expected for the GP_{Set1} . This difference seems to be negligible, but let focus now on the expected cost rate.

Based on the optimal ages of replacement and Eq. 11, the expected cost rate for each degradation process was determined and depicted in Fig. 9. Note that there is a difference of at most 200

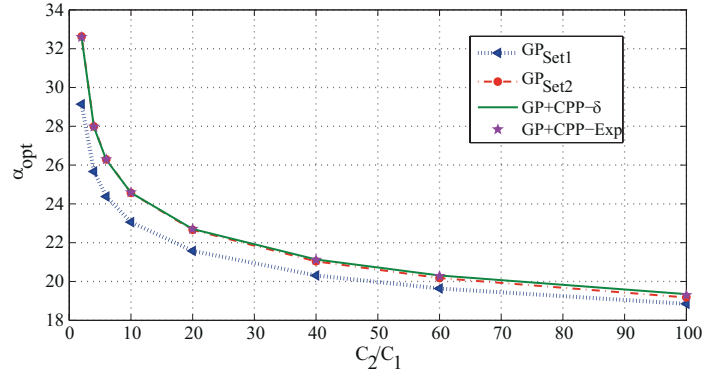


Figure 8: Optimal replacement ages in years vs C_2/C_1 .

USD/Joint between the GP_{Set1} with the other degradation processes and an average difference of 50 USD/Joint between the Mixed Processes with the GP_{Set2} . Considering that a pipeline may have more than 3,000 joints, this difference would represent an increase near 600,000 USD for the GP_{Set1} and 150,000 USD for the GP_{Set2} . Therefore, this difference is nothing but negligible and it illustrates how difficult is a maintenance decision-making process. Note that although the expected cost rates for the mixed processes are slightly shorter than the GP_{Set2} , their optimal ages of replacement are almost the same. The proposed approach can be used to support intervention decisions aiming to reduce investments in pipeline interventions and possible failures.

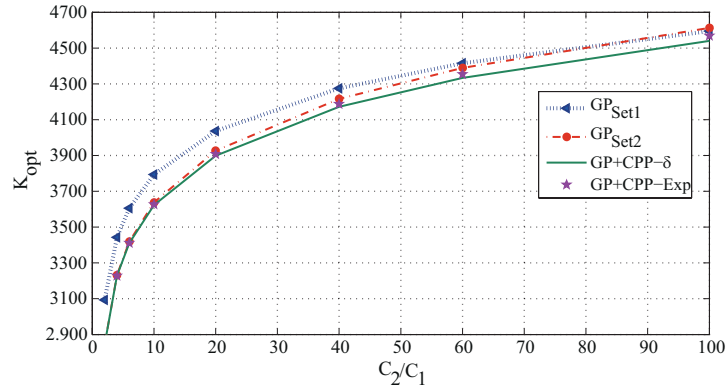


Figure 9: Optimal cost in USD per unit time.

For instance, the cumulative failure distribution can be estimated up to each of the optimal ages of replacement not only to describe the decision following a cost-based approach but also to consider the probability of a future loss of containment on the pipe. Fig. 10 presents this estimation from the illustrative example, where a clear decreasing performance is depicted, once the failure or corrective cost grows. This tendency is expected because the optimal age of replacement is reduced, so more frequent intervention takes place. However, this figure provides additional information about possible optimal ages that fit a similar ALARP (*As Low As Reasonably Practicable*) perspective. Although the cost of failure increases significantly, in comparison

to the maintenance cost, the failure probability yields an almost stable point, regardless inspections are implemented reiteratively when $C_2/C_1 > 20$. Depending on the company maintenance policy, these results are useful to improve maintenance planning.

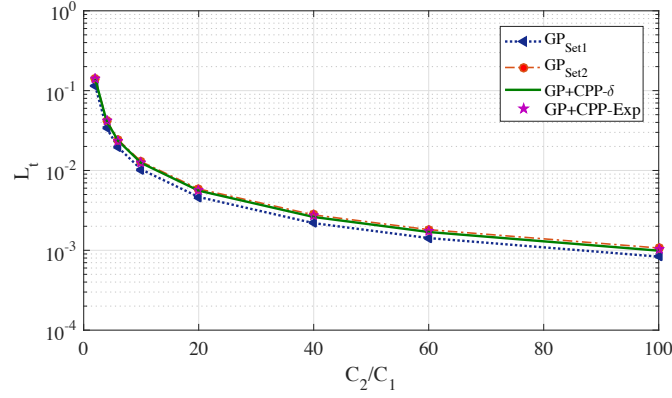


Figure 10: Cumulative failure distribution until α_{opt} .

7. Conclusions

A stochastic characterization of a corroded pipeline is presented in this paper based on a ILI (In-Line) inspections of a real pipeline using a Mixed Lévy Process composed by a Gamma and a Compound Poisson Processes. An optimization approach was proposed to estimate the parameters of this mixed process considering location uncertainties and a significant amount of detected defects. The results from the degradation process were then implemented in an integrity assessment based on the Mean Time to Failure (MTTF) along the pipeline and a maintenance approach following an *Age of replacement model*.

This characterization aims to fit the mean and central moments of the reported degradation. The results produced relevant differences with a simple Gamma Process (GP_{Set2}) in the optimal replacement ages, which in turn, correspond to an increase about 150,000 USD in the expected cost rate for a pipeline with 3,000 joints. Regarding the integrity assessment, the MTTF helped identifying leak-prone segments of the pipeline, which in turn, were compared with the potential spill volume to recognize critical locations. These assessments seek to support a decision-making process regarding a pipeline intervention plan.

The proposed approach is a complementary alternative for codes/standards such as API 579-1/ASME FFS-1 for corroded pipeline assessments. A stochastic approach allows decision makers to obtain results that capture the underlying uncertainties of the complex degradation model.

Acknowledgments

R. Amaya-Gómez thanks the National Department of Science, Technology and Innovation of Colombia for the PhD scholarship (COLCIENCIAS Grant No. 727, 2015) and Campus France for the Eiffel Excellence Program (2018).

Bibliography

- [1] CONCAWE, Performance of European cross-country oil pipelines. Statistical summary of reported spillages in 2012 and since 1971, Tech. rep., Conservation of Clean Air and Water in Europe, online; accessed February 2015 (2013).
- [2] US DoT PHMSA, Data and Statistics, <http://www.phmsa.dot.gov/pipeline/library/data-stats>, online; accessed February 2015 (2015).
- [3] P. Tang, J. Yang, J. Zheng, I. Wong, S. He, J. Ye, G. Ou, Failure analysis and prediction of pipes due to the interaction between multiphase flow and structure, *Engineering Failure Analysis* 16 (5) (2009) 1749 – 1756. doi:<http://dx.doi.org/10.1016/j.engfailanal.2009.01.002>.
- [4] G. Zhang, L. Zeng, H. Huang, X. Guo, A study of flow accelerated corrosion at elbow of carbon steel pipeline by array electrode and computational fluid dynamics simulation, *Corrosion Science* 77 (2013) 334 – 341. doi:<http://dx.doi.org/10.1016/j.corsci.2013.08.022>.
- [5] R. Amaya-Gómez, M. Sánchez-Silva, F. Muñoz, Pattern recognition techniques implementation on data from In-Line Inspection (ILI), *Journal of Loss Prevention in the Process Industries* 44 (2016) 735 – 747. doi:<http://dx.doi.org/10.1016/j.jlp.2016.07.020>.
- [6] M. Pandey, D. Lu, Estimation of parameters of degradation growth rate distribution from noisy measurement data, *Structural Safety* 43 (2013) 60 – 69. doi:<http://dx.doi.org/10.1016/j.strusafe.2013.02.002>.
- [7] S. Zhang, W. Zhou, Cost-based optimal maintenance decisions for corroding natural gas pipelines based on stochastic degradation models, *Engineering Structures* 74 (2014) 74 – 85. doi:<http://dx.doi.org/10.1016/j.engstruct.2014.05.018>.
- [8] F. Bazán, A. Beck, Stochastic process corrosion growth models for pipeline reliability, *Corrosion Science* 74 (2013) 50 – 58. doi:<http://dx.doi.org/10.1016/j.corsci.2013.04.011>.
- [9] S. Li, S. Yu, H. Zeng, J. Li, R. Liang, Predicting corrosion remaining life of underground pipelines with a mechanically-based probabilistic model, *Journal of Petroleum Science and Engineering* 65 (34) (2009) 162 – 166. doi:<http://dx.doi.org/10.1016/j.petrol.2008.12.023>.
- [10] F. Caleyó, J. Velázquez, A. Valor, J. Hallen, Probability distribution of pitting corrosion depth and rate in underground pipelines: A Monte Carlo study, *Corrosion Science* 51 (9) (2009) 1925 – 1934. doi:<http://dx.doi.org/10.1016/j.corsci.2009.05.019>.
- [11] NORSOK, CO₂ corrosion rate calculation model, Tech. rep., Oslo, Norway (1998).
- [12] C. de Waard, U. Lotz, Prediction of CO₂ corrosion of carbon steel, in: NACE International, Houston, United States, 1993.
- [13] NACE International, RP0502-2002 Pipeline External Corrosion Direct Assessment Methodology. Standard Recommended Practice, Tech. rep., Houston, USA (2002).
- [14] A. Barbian, M. Beller, In-Line Inspection of High Pressure Transmission Pipelines: State-of-the-Art and Future Trends, in: 18th World Conference on Nondestructive Testing, Durban, South Africa, 2012.
- [15] Y. Sahraoui, R. Khelif, A. Chateaneuf, Maintenance planning under imperfect inspections of corroded pipelines, *International Journal of Pressure Vessels and Piping* 104 (2013) 76 – 82. doi:<http://dx.doi.org/10.1016/j.ijvp.2013.01.009>.
- [16] W. Gomes, A. Beck, Optimal inspection and design of onshore pipelines under external corrosion process, *Structural Safety* 47 (2014) 48 – 58. doi:<http://dx.doi.org/10.1016/j.strusafe.2013.11.001>.
- [17] C. Ossai, B. Boswell, I. Davies, Stochastic modelling of perfect inspection and repair actions for leak-failure prone internal corroded pipelines, *Engineering Failure Analysis* 60 (2016) 40 – 56. doi:<http://dx.doi.org/10.1016/j.engfailanal.2015.11.030>.
- [18] H. Hong, Inspection and maintenance planning of pipeline under external corrosion considering generation of new defects, *Structural Safety* 21 (3) (1999) 203 – 222. doi:[http://dx.doi.org/10.1016/S0167-4730\(99\)00016-8](http://dx.doi.org/10.1016/S0167-4730(99)00016-8).
- [19] F. Caleyó, J. Velázquez, A. Valor, J. Hallen, Markov chain modelling of pitting corrosion in underground pipelines, *Corrosion Science* 51 (9) (2009) 2197 – 2207. doi:<http://dx.doi.org/10.1016/j.corsci.2009.06.014>.
- [20] W. Zhou, H. Hong, S. Zhang, Impact of dependent stochastic defect growth on system reliability of corroding pipelines, *International Journal of Pressure Vessels and Piping* 96 and 97 (2012) 68 – 77. doi:<http://dx.doi.org/10.1016/j.ijvp.2012.06.005>.
- [21] R. Nicolai, R. Dekker, J. van Noordwijk, A comparison of models for measurable deterioration: An application to coatings on steel structures, *Reliability Engineering & System Safety* 92 (12) (2007) 1635 – 1650, special Issue on {ESREL} 2005. doi:<http://dx.doi.org/10.1016/j.ress.2006.09.021>.
- [22] D. Frangopol, M.-J. Kallen, J. van Noordwijk, Probabilistic models for life-cycle performance of deteriorating structures: review and future directions, *Progress in Structural Engineering and Materials* 6 (4) (2004) 197–212. doi:10.1002/pse.180.
- [23] M. Abdel-Hameed, *Lévy Processes and Their Applications in Reliability and Storage*, Springer-Verlag Berlin Heidelberg, 2014. doi:10.1007/978-3-642-40075-9.

- [24] J. Riascos-Ochoa, M. Sánchez-Silva, G.-A. Klutke, Modeling and reliability analysis of systems subject to multiple sources of degradation based on Lévy processes, *Probabilistic Engineering Mechanics* 45 (2016) 164 – 176. doi:<http://dx.doi.org/10.1016/j.probenmech.2016.05.002>.
- [25] POF, Specifications and requirements for intelligent pig inspection of pipelines, Tech. rep., Pipeline Operators Forum (2008).
- [26] B. Eiber, Overview of Integrity Assessment Methods for Pipelines, Tech. rep., Robert J. Eiber Consultant Inc (2003).
URL <http://mrsc.org/getmedia/8B8FF358-4055-4D0E-9ED6-08AE41DA68B7/EiberOverview.aspx>
- [27] K. Reber, M. Beller, Ultrasonic in-line inspection tools to inspect older pipelines for cracks in girth and long-seam welds, in: *Pigging and service association seminar*, Aberdeen, Scotland, 2003.
- [28] M. Pandey, Probabilistic models for condition assessment of oil and gas pipelines, *NDT & E International* 31.
- [29] S. Kuniewski, J. van der Weide, J. van Noortwijk, Sampling inspection for the evaluation of time-dependent reliability of deteriorating systems under imperfect defect detection, *Reliability Engineering & System Safety* 94 (9) (2009) 1480 – 1490, eSREL 2007, the 18th European Safety and Reliability Conference. doi:<https://doi.org/10.1016/j.ress.2008.11.013>.
- [30] H. Qin, Probabilistic Modeling and Bayesian Inference of Metal-Loss Corrosion with Application in Reliability Analysis for Energy Pipelines, Master's thesis, electronic Thesis and Dissertation Repository. Paper 2246. (2014).
- [31] S. Zhang, W. Zhou, H. Qin, Inverse Gaussian process-based corrosion growth model for energy pipelines considering the sizing error in inspection data, *Corrosion Science* 73 (2013) 309 – 320. doi:<http://dx.doi.org/10.1016/j.corsci.2013.04.020>.
- [32] M. Sánchez-Silva, G.-A. Klutke, Reliability and life-cycle analysis of deteriorating systems, Springer series in Reliability Engineering, Springer, 2016.
- [33] M. Sánchez-Silva, G. Klutke, D. Rosowsky, Life-cycle performance of structures subject to multiple deterioration mechanisms, *Structural Safety* 33 (3) (2011) 206 – 217. doi:<http://dx.doi.org/10.1016/j.strusafe.2011.03.003>.
- [34] H. Qin, W. Zhou, S. Zhang, Bayesian inferences of generation and growth of corrosion defects on energy pipelines based on imperfect inspection data, *Reliability Engineering & System Safety* 144 (2015) 334 – 342. doi:<http://dx.doi.org/10.1016/j.ress.2015.08.007>.
- [35] S. Zhang, W. Zhou, System reliability of corroding pipelines considering stochastic process-based models for defect growth and internal pressure, *International Journal of Pressure Vessels and Piping* 111-112 (2013) 120 – 130. doi:<http://dx.doi.org/10.1016/j.ijpvp.2013.06.002>.
- [36] J. van Noortwijk, A survey of the application of gamma processes in maintenance, *Reliability Engineering & System Safety* 94 (1) (2009) 2 – 21, maintenance Modeling and Application. doi:<http://dx.doi.org/10.1016/j.ress.2007.03.019>.
- [37] J. van Noortwijk, M. Pandey, A stochastic deterioration process for time-dependent reliability analysis, in: *Eleventh IFIP WG 7.5 Working Conference on Reliability and Optimization of Structural Systems*, Banff, Canada, 2004.
- [38] N. Chen, Z.-S. Ye, Y. Xiang, L. Zhang, Condition-based maintenance using the inverse Gaussian degradation model, *European Journal of Operational Research* 243 (1) (2015) 190 – 199. doi:<https://doi.org/10.1016/j.ejor.2014.11.029>.
- [39] H. Qin, S. Zhang, W. Zhou, Inverse Gaussian process-based corrosion growth modeling and its application in the reliability analysis for energy pipelines, *Frontiers of Structural and Civil Engineering* 7 (3) (2013) 276–287. doi:[10.1007/s11709-013-0207-9](https://doi.org/10.1007/s11709-013-0207-9).
- [40] W. Zhou, W. Xiang, H. Hong, Sensitivity of system reliability of corroding pipelines to modeling of stochastic growth of corrosion defects, *Reliability Engineering & System Safety* 167 (2017) 428 – 438, special Section: Applications of Probabilistic Graphical Models in Dependability, Diagnosis and Prognosis. doi:<http://dx.doi.org/10.1016/j.ress.2017.06.025>.
- [41] W. Peng, Y.-F. Li, Y.-J. Yang, H.-Z. Huang, M. Zuo, Inverse Gaussian process models for degradation analysis: A Bayesian perspective, *Reliability Engineering & System Safety* 130 (2014) 175 – 189. doi:<https://doi.org/10.1016/j.ress.2014.06.005>.
- [42] J. Riascos-Ochoa, The Lévy-based framework for deterioration modeling, reliability estimation and maintenance of engineered systems, Ph.D. thesis, Universidad de los Andes, unpublished Thesis (2016).
- [43] H. A. Kishawy, H. A. Gabbar, Review of pipeline integrity management practices, *International Journal of Pressure Vessels and Piping* 87 (7) (2010) 373 – 380. doi:<http://dx.doi.org/10.1016/j.ijpvp.2010.04.003>.
- [44] R. Amaya-Gómez, M. Sánchez-Silva, E. Bastidas-Arteaga, F. Schoefs, F. Mu noz, Reliability assessments of corroded pipelines based on internal pressure A review, *Engineering Failure Analysis* doi:<https://doi.org/10.1016/j.engfailanal.2019.01.064>.
- [45] J. Fontecha, N. Cano, N. Velasco, F. Mu noz, Optimal sectioning of hydrocarbon transport pipeline by volume minimization, environmental and social vulnerability assessment, *Journal of Loss Prevention in the Process Industries* 44 (2016) 681 – 689. doi:<https://doi.org/10.1016/j.jlp.2016.07.017>.

Appendix A. Estimation of degradation parameters

GP and IGP processes

The parameters of the gamma distribution can be determined using the method of moments described in [37]. This method uses the mean and variance of the degradation process, to determine the c parameter from the shape function $v(t) = ct^b$ and the constant scale parameter u . If the power b is known, this non-stationary GP can be transformed into a stationary degradation process by the map $z = t^b$. Otherwise, this parameter could be determined numerically by the method of Maximum Likelihood [21]. As a result of the method of moments, the estimate of these parameters (i.e., \hat{c} and \hat{u}) can be obtained using the time between inspections $w_j = (t_j - t_{j-1})$, the degradation of each defect x_j^i , and defect-depth increments $\delta_j^i = (x_j^i - x_{j-1}^i)$ with $t_0 = 0$ [37]:

$$\frac{\hat{c}}{\hat{u}} = \frac{\sum_{j=1}^n \delta_j^i}{\sum_{j=1}^n w_j} = \frac{x_n^i}{t_n} := \bar{\delta}_i, \quad \frac{x_n^i}{\hat{u}} \left(1 - \frac{\sum_{j=1}^n w_j^2}{[\sum_{j=1}^n w_j]^2} \right) = \sum_{j=1}^n (\delta_j^i - \bar{\delta}_i w_j)^2 \quad (\text{A.1})$$

Moreover, in a reliability-based pipeline integrity assessment it is common to assume a linear growth of the corrosion rate (i.e., $b = 1$) because of its simplicity [20]. Considering that pipeline inspections are carried out periodically every 2 to 4 years, these expressions can be simplified using a constant inspection interval τ as follows:

$$\frac{\hat{c}}{\hat{u}} = \bar{\delta}_i, \quad \frac{x_n^i}{\hat{u}} \left(1 - \frac{1}{n} \right) = n\tau^2 \bar{\delta}_i^2 - 2\bar{\delta}_i \tau x_n^i + \sum_{j=1}^n (\delta_j^i)^2 \quad (\text{A.2})$$

In case only two ILI inspections are considered in an homogeneous case (i.e., $b = 1$), this procedure is simplified as follows:

$$c = \frac{\mathbb{E}[X_t]^2}{t \cdot \text{Var}[X_t]}, \quad u = \frac{\mathbb{E}[X_t]}{\text{Var}[X_t]} \quad (\text{A.3})$$

Similar results can be obtained for the IGP process, which variance and coefficient of variation are given as follow:

$$\text{Var}[X_t] = \frac{\Lambda_t}{\zeta}, \quad \text{COV}[X_t] = \frac{1}{\sqrt{\zeta \Lambda_t}}$$

In this case, the parameters $\Lambda_t = \Lambda_0 t$ and ζ are given by:

$$\Lambda_0 = \frac{\mathbb{E}[X_t]}{t}, \quad \zeta = \frac{\mathbb{E}[X_t]}{\text{Var}[X_t]} \quad (\text{A.4})$$

The mean and the variance of both stochastic processes are summarized in Table A.6.

Table A.6: GP and IGP mean and variance [31, 36]

Process	Mean	Variance
GP	$E[X_t] = \frac{v(t)}{u}$	$\text{Var}[X_t] = \frac{v(t)}{u^2}$
IGP	$E[X_t] = \Lambda_t$	$\text{Var}[X_t] = \frac{\Lambda_t}{\zeta}$